

AMMRC PTR 71-3

AD

AD 732893

MODIFICATIONS TO AN AXIAL TENSION TESTER FOR BRITTLE MATERIALS

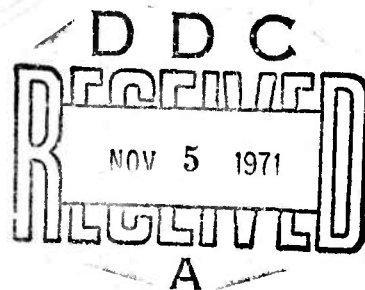
GEORGE W. DRISCOLL and FRANCIS I. BARATTA
THEORETICAL & APPLIED MECHANICS RESEARCH LABORATORY

August 1971

Approved for public release; distribution unlimited.

Reproduced by
NATIONAL TECHNICAL
INFORMATION SERVICE
Springfield, Va. 22151

ARMY MATERIALS AND MECHANICS RESEARCH CENTER
Watertown, Massachusetts 02172



ACCESSION #	
CFSTI	WHITE SECTION <input checked="" type="checkbox"/>
DDG	BUFF SECTION <input type="checkbox"/>
UNCLASSIFIED	<input type="checkbox"/>
INSTRUCTIONS	
BY	
DISTRIBUTION/AVAILABILITY CODES	
REST.	STATE. UNCLAS. SPECIAL
A	

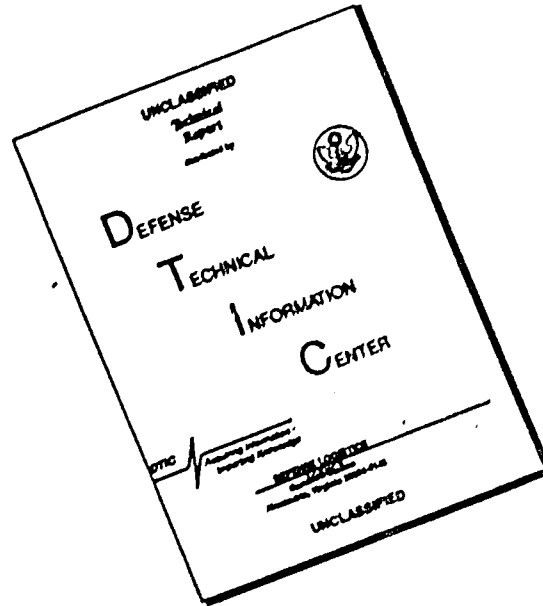
The findings in this report are not to be construed as an official Department of the Army position, unless so designated by other authorized documents.

Mention of any trade names or manufacturers in this report shall not be construed as advertising nor as an official indorsement or approval of such products or companies by the United States Government.

DISPOSITION INSTRUCTIONS

Destroy this report when it is no longer needed.
Do not return it to the originator.

DISCLAIMER NOTICE



THIS DOCUMENT IS BEST QUALITY AVAILABLE. THE COPY FURNISHED TO DTIC CONTAINED A SIGNIFICANT NUMBER OF PAGES WHICH DO NOT REPRODUCE LEGIBLY.

UNCLASSIFIED

Security Classification

DOCUMENT CONTROL DATA - R&D		
<i>(Security classification of title, body of abstract and indexing annotation must be entered when the overall report is classified)</i>		
1. ORIGINAL ACTIVITY (Corporate author) Army Materials and Mechanics Research Center Watertown, Massachusetts 02172	2a. REPORT SECURITY CLASSIFICATION Unclassified	
	2b. GROUP	
3. REPORT TITLE MODIFICATIONS TO AN AXIAL TENSION TESTER FOR BRITTLE MATERIALS		
4. DESCRIPTIVE NOTES (Type of report and inclusive dates) Product Technical Report		
5. AUTHOR(S) (First name, middle initial, last name) George W. Driscoll and Francis I. Baratta		
6. REPORT DATE August 1971	7a. TOTAL NO. OF PAGES 22	7b. NO. OF REFS 7
8a. CONTRACT OR GRANT NO. b. Project No. PEMA c. AMC Code 49310MS042 d.	9a. ORIGINATOR'S REPORT NUMBER(S) AMMRC PTR 71-3	
	9b. OTHER REPORT NO(S) (Any other numbers that may be assigned this report)	
10. DISTRIBUTION STATEMENT Approved for public release; distribution unlimited.		
11. SUPPLEMENTARY NOTES	12. SPONSORING MILITARY ACTIVITY U. S. Army Materiel Command Washington, D. C. 20315	
13. ABSTRACT <p>In the conclusions of an earlier report, the authors expressed their intent to further develop a system for the tension testing of brittle materials. This report investigates the steps taken to accomplish this objective. A redesign of the original device has produced a more compact, easier to use system while still maintaining all the favorable features. This device effectively minimizes the parasitic bending stress normally associated with the conventional tension test. Additionally, the specimen designed for use in the original device was redesigned to reduce the overall size and to incorporate a constant diameter gage section.</p> <p>A plastic material (Hysol cp5-4290), which was readily available and which exhibits the brittle characteristics desired, was chosen as the specimen material to be used in the test program conducted to proof test the device and specimen design. Tests were also conducted to determine the load-error effect of the O-rings with the intent of establishing a load calibration procedure.</p>		

DD FORM 1473
1 NOV 65

UNCLASSIFIED
Security Classification

UNCLASSIFIED

Security Classification

14. KEY WORDS	LINK A		LINK B		LINK C	
	ROLE	WT	ROLE	WT	ROLE	WT
Brittleness Tension tests Materials tests Tension testers Mechanical tests Tensile strength						

UNCLASSIFIED

Security Classification

AMMRC PTR 71-3

MODIFICATIONS TO AN AXIAL TENSION TESTER FOR BRITTLE MATERIALS

Product Technical Report by

GEORGE W. DRISCOLL and FRANCIS I. BARATTA

August 1971

Project PEMA
AMC Code 49310M5042
Materials Testing Technology

Approved for public release; distribution unlimited.

THEORETICAL & APPLIED MECHANICS RESEARCH LABORATORY
ARMY MATERIALS AND MECHANICS RESEARCH CENTER
Watertown, Massachusetts 02172

ARMY MATERIALS AND MECHANICS RESEARCH CENTER

MODIFICATIONS TO AN AXIAL TENSION TESTER FOR BRITTLE MATERIALS

ABSTRACT

In the conclusions of an earlier report, the authors expressed their intent to further develop a system for the tension testing of brittle materials. This report investigates the steps taken to accomplish this objective. A redesign of the original device has produced a more compact, easier to use system while still maintaining all the favorable features. This device effectively minimizes the parasitic bending stress normally associated with the conventional tension test. Additionally, the specimen designed for use in the original device was redesigned to reduce the overall size and to incorporate a constant diameter gage section.

A plastic material (Hysol cp5-4290), which was readily available and which exhibits the brittle characteristics desired, was chosen as the specimen material to be used in the test program conducted to proof test the device and specimen design. Tests were also conducted to determine the load-error effect of the O-rings with the intent of establishing a load calibration procedure.

CONTENTS

	Page
ABSTRACT	
LIST OF SYMBOLS	
I. INTRODUCTION.	1
II. BACKGROUND.	1
III. DESIGN OF TESTING DEVICE AND SPECIMEN	3
IV. SYSTEM ERROR SOURCES.	3
V. LOAD CALIBRATION PROCEDURE.	5
VI. TEST PROGRAM.	5
1. Test Procedure.	5
2. Test Results.	7
3. Analysis of Test Results.	8
VII. CONCLUSIONS	9
APPENDIX A - SYSTEM ERRORS.	10
APPENDIX B - TEST DEVICE AND SPECIMEN	16
APPENDIX C - TEST EQUIPMENT AND MEASUREMENT SYSTEM.	19
LITERATURE CITED.	20

LIST OF SYMBOLS

C_p	Pressure center
D	Diameter at large end of specimen (inches)
d	Minimum diameter of the specimen gage section (inches)
E_c	Modulus of elasticity in compression (psi)
E_e	Error caused by the eccentricity between D and d
E_T	Modulus of elasticity in tension (psi)
e	Eccentricity between D and d before loading (inches)
e_t	Total eccentricity between d and C_p after loading (inches)
I	Moment of inertia (inches) ⁴
k	Calibration constant
l	Effective length (inches)
M	Bending moment (pound-inches)
n	Number of specimens
P	Axial load on diameter d (pounds)
p	Applied hydrostatic pressure (psi)
P_f	Recorded pressure at fracture (psi)
q	Ratio of tensile strength to compressive strength
S_σ	Standard or root-mean-square deviation of σ_T
V_σ	Coefficient of variance of σ_T (percent)
x	Distance from the origin of the coordinates
y	Displacement at distance x
\bar{y}	Centerline distance between C_p and D (inches)
X, Y	Rectangular coordinates
δ	Displacement of d caused by load P (inches)
$\Delta\sigma$	Stress difference ratio (psi)

ϵ_d Axial strain in dummy specimen (inches/inch)

ϵ_p Predicted axial strain in specimen (inches/inch)

ϵ_s Axial strain in specimen (inches/inch)

ν Poisson's ratio

σ_b Bending stress in diameter d caused by load P (psi)

σ_c Compressive stress (psi)

σ_p Applied hydrostatic pressure (psi)

σ_T Tensile strength (psi)

$\bar{\sigma}_T$ Average tensile strength (psi)

σ_{Ti} Individual tensile strength values (psi)

σ_x Axial stress in gage length diameter of specimen and dummy specimen (psi)

σ_y Stress in y coordinate direction (psi)

σ_z Stress in z coordinate direction (psi)

ϕ Internal friction angle (degrees)

I. INTRODUCTION

In today's world, the applications of brittle materials such as ceramics, cermets, graphite, glass, etc., in structures are becoming more numerous and often critical; therefore, it is imperative to possess accurate knowledge of the mechanical property data. The tensile testing of ductile materials has been standardized for many years resulting in accurate, valid data. Many times when conducting these tests, a misalignment in the load train exists which imposes a bending stress on the test specimen. Within reasonable limits this is permissible without jeopardizing the accuracy of the test data because of the inherent characteristic of a ductile material which allows the material to deform locally and permits the specimen to realign itself. Unlike a ductile material, bending stresses imposed on a brittle material specimen can lead to gross errors in the data and, therefore, the need for an accurate, but simple, method for an uniaxial tension test becomes very apparent.

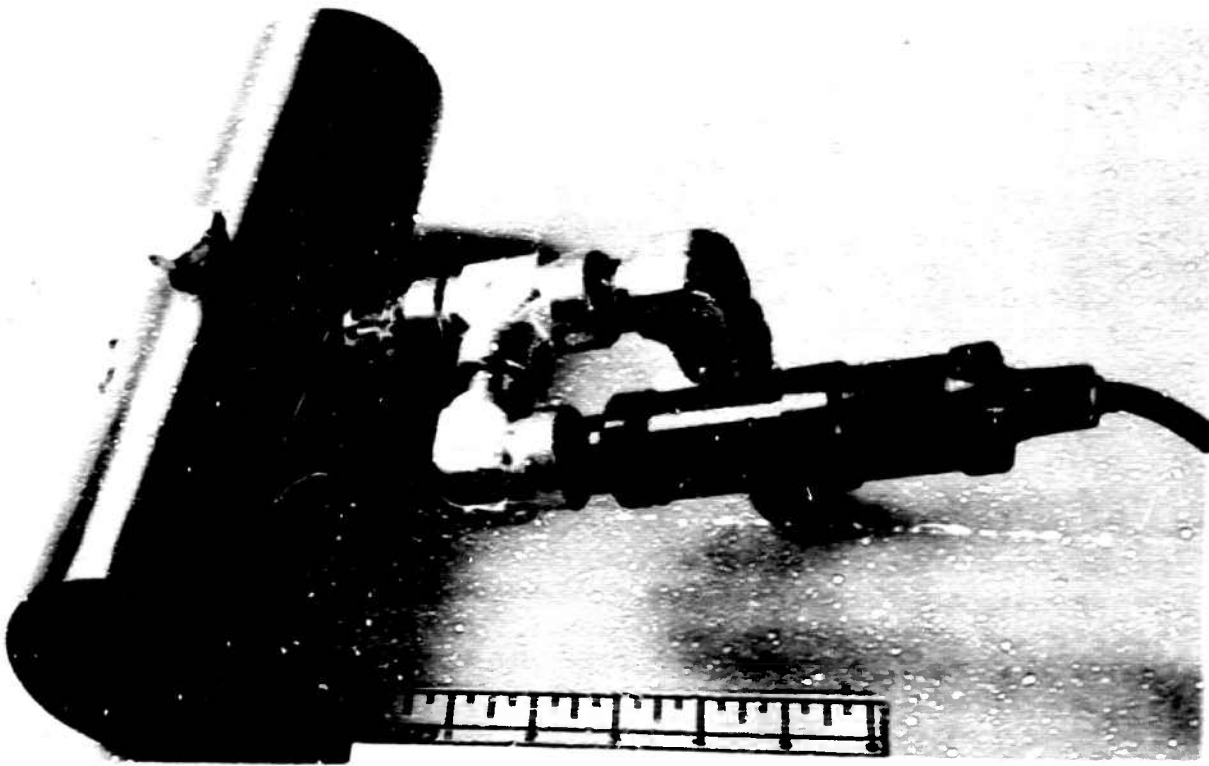
Methods for brittle material testing have been proposed such as the burst test¹ wherein a hydrostatic pressure is applied to the inside of a short thin-walled specimen through the medium of an elastic envelope. Tensile strength is determined from the knowledge of the pressure at failure and specimen dimensions. Another proposed method for testing of brittle materials is the gas bearing facilities² wherein precise alignment of the load train is maintained through precision bearings which float on a film of gas. At the Army Materials and Mechanics Research Center, an accurate method³ was proposed for the uniaxial tension testing of brittle materials. Further development of the unique testing device and test specimen used in this method has been accomplished and is the subject of this report.

II. BACKGROUND

In a report by Baratta and Driscoll³, a test method for the tensile testing of brittle materials was proposed. The test device used was a simple, inexpensive design shown in Figures 1 and 2 and referred to as the BATT (Brittle Axial Tension Tester). The test specimen designed to be used in the BATT is shown in Figure 3. Basically, the BATT is a cylinder with two O-rings retained in grooves at a predetermined distance. Upon inserting the test specimen into the BATT, the O-rings engage and form a seal around the larger end diameters of the specimen. Hydraulic pressure applied to the end diameters of the specimen through a port in the middle of the cylinder produces an axial-tensile force in the specimen gage section. Continuous monitoring of the pressure is maintained up to specimen failure. The tensile strength (σ_T) of the material is based on the minimum cross-sectional area of the specimen and is calculated from conditions of equilibrium using the following equation:

$$\sigma_T = p_f \left[\left(\frac{D}{d} \right)^2 - 1 \right] k \quad (1)$$

where k is a calibration constant combining the load-loss factor and the stress concentration factor at diameter d caused by the varying gage section diameter.



19-085-162/AM7-67

Figure 1. BATT (Bristle Axial Tension Tester)

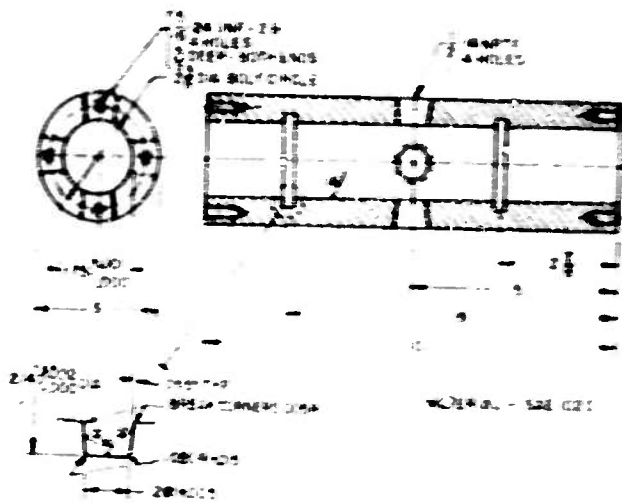
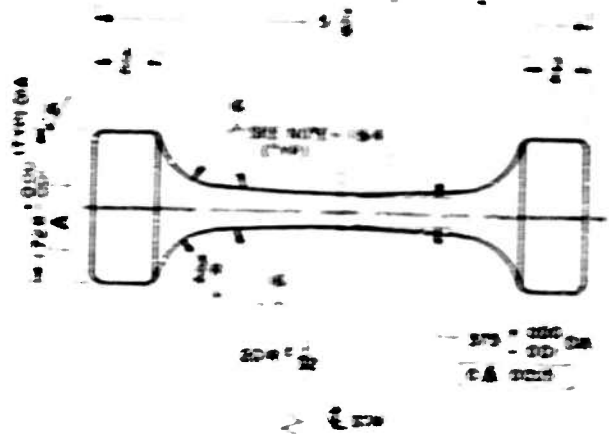


Figure 2. BATT cylinder



NOTE

- 1 GRIP FINISH MARKS TO BE IN PLANE OF GAUGE LENGTH APPROX 1/8 INCH DISTANCE EACH SIDE OF TENDENCY
- 2 BREAK ALL CORNERS 2R
- 3 CENTERS PERMISSIBLE
- 4 NO DISCONTINUITY ALLOWED ALONG 2.4 DIA AT TENDENCY POINT

Figure 3. Torsion test specimen configuration

An assumption is made that the stress is constant across the cross-section area at d . Bending of the specimen is effectively minimized because of the flexibility of the O-rings and the quality control of the manufacturing process which holds the eccentricity existing between diameters of the specimen to a close tolerance. At the time of the earlier research, it became apparent that a continued investigation of certain design changes to the test device and specimen could improve their proposed testing method. The conclusions of the report made note of this. Although it did not inhibit the earlier investigation, it was realized that a reduced size specimen with a constant diameter gage section would be the optimum design for future testing. Changes considered would include a redesign of the device to accommodate the specimen design changes and also provide an improved means of placing the specimen into the cylinder. With the earlier design, the possibility of breaking a specimen as it was inserted through the O-rings was always present. The need to further investigate the effect of friction between the O-rings of the BATT and the test specimen and to establish a procedure for determining the true tensile load applied to the test specimen was also foreseen.

III. DESIGN OF TESTING DEVICE AND SPECIMEN

The design requirements of an ideal brittle-material tension-test system are: (1) that only a uniaxial tensile force be applied to the gage section of the test specimen and (2) that an expeditious determination of the uniaxial stress condition can be made. In the conventional test method, the major source of error arises from an unintentionally applied bending force usually produced through: a misalignment in the load train, asymmetrical contact between the specimen and holding device, an inherent eccentricity in the specimen between the axes of the gage section and the ends where the load is applied, etc. Although the elimination of all forces contributing to bending stresses is not practical, the employment of a test system which minimizes the eccentric forces transferred to the test specimen and the utilization of a test specimen wherein eccentricity has been kept to a minimum will control these forces to a tolerable degree.

The test device and specimen (Figures 4 and 5) proposed here meet the requirements set forth in the preceding paragraph in a practical sense. The flexibility of the O-rings permits the alignment of the specimen in the test device without the imposition of bending forces; and since the applied load to the specimen is made through a fluid medium, parasitic bending stresses can be effectively minimized by controlled manufacture of the specimen. Determination of the stress condition can be readily obtained through a force-equilibrium consideration. It is possible that small errors may exist in this proposed system. Such errors are enumerated in the following section.

IV. SYSTEM ERROR SOURCES

Possible sources of error that could exist in the system are:

1. Bending caused by an eccentricity between the gage-section diameter and the end diameters of the specimen, or by an imposed bending force created by the insertion of the specimen into the device.

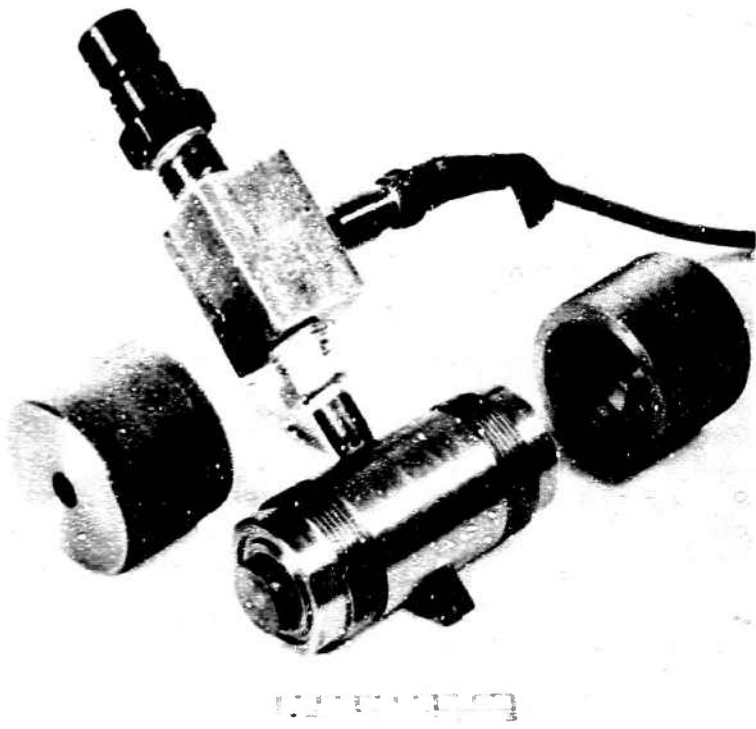


Figure 4. Test device (end caps removed to show specimen in test position)

19-066-450/AMC-70

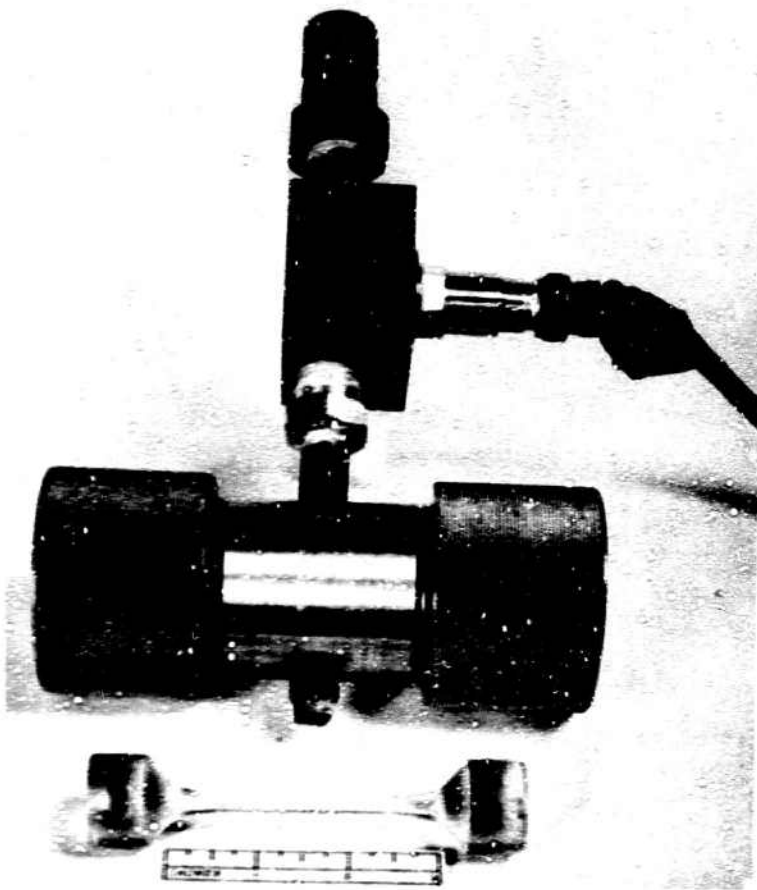


Figure 5. Assembled test fixture and test specimen

19-066-451/AMC-70

Results of tests indicated an error of less than 2-1/2 percent.

2. Load loss through the contact between the O-rings and specimen. Results indicated an error of 1-1/2 percent to 3 percent for the material tested.

3. A triaxial stress state where uniaxial stress is assumed could create an error of 4 percent or less.

See Appendix A for a detailed discussion of system errors.

V. LOAD CALIBRATION PROCEDURE

A load calibration procedure was established for the determination of the O-ring load loss. Appendix A contains a detailed discussion of this procedure.

VI. TEST PROGRAM

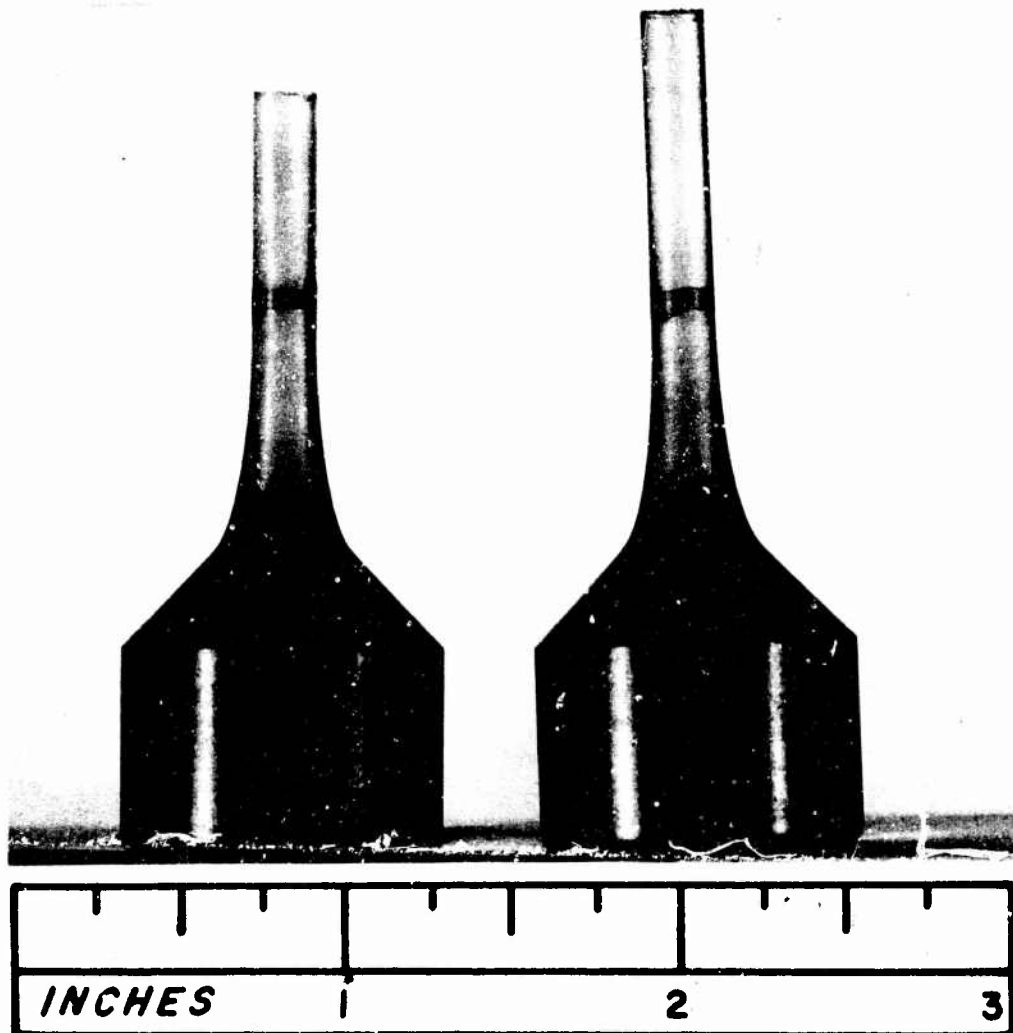
1. Test Procedure

The primary objective of the test program was to proof test the test device and specimen designs; therefore, only that quantity of specimens necessary to determine the adequacy of the system was manufactured and tested. If tensile-strength values for design purposes were desired, it would be advisable to test a larger quantity of specimens than was tested here.

Twelve specimens were manufactured from 1-1/4-inch diameter hysol cp5-4290 material to the design shown in Figure B3. Selection of this plastic material was made because of its brittle material characteristics which exhibit the typical transverse fracture in tension (Figure 6*) and the high degree of sensitivity to discontinuities. Some difficulty was experienced in machining a constant diameter throughout the gage section length. Although the variation was small, usually less than 0.002 inch, the minimum diameter in some cases did locate close to the tangent point of the fillet. Preliminary tests had indicated that failure generally occurred across the minimum diameter. It was most desirable to contain the fracture close to the middle of the gage section length; therefore, the gage section length of each specimen was polished to provide a slight tapering of approximately 0.001 inch to a minimum diameter in the region of the middle of the gage length. The stress concentration arising from this contour is effectively negligible. All of the specimens were inspected for compliance with the specified dimensions, and a record was made of the reduced diameter d , the end diameters D , and the total eccentricity e .

Not all the specimens met the eccentricity requirement specified (Table I), but this did not introduce any appreciable error in the results. (See Appendix A, para. A2.) Establishment of the stress rate for the test specimens was made by the following procedure: O-rings were fitted to each end face of the test device

*The tangency between the gage section diameter and the elliptical fillet were accentuated with a dark line to indicate the gage section length.



19-066-620/AMC-70

Figure 6. Transverse fracture, typical of brittle materials

cylinder, and the end caps were assembled to the cylinder. All open ports in the test device were sealed with pipe plugs. (See Appendix C for test equipment and measuring system used.) Adjustment of the pressurizing rate to correspond to a stress rate of approximately 800 psi/sec for the specimen was made through a series of time-pressure curves recorded on a Moseley X-Y recorder. This stress-rate value was chosen because it approximated the magnitude recommended by ASTM for static tension testing and was also used in the testing of the BATT. The procedure outline in Appendix B, para. 1 was followed by each specimen preparatory to testing. During the test, pressure data were continuously recorded up to specimen fracture on a Moseley X-Y recorder calibrated for time on the Y-axis and pressure on the X-axis. Prior to each test, the X-Y recorder was calibrated (see Appendix C, para. C2).

Table I.

Specimen No.	Eccentricity (e) Inches	Pressure At Fracture (p_f) psi	Tensile Strength (σ_{Ti}) psi*
1	0.0005	508.5	11880
2	0.0005	550.0	13220
3	0.0005	513.5	12364 (data not used)
4	0.0002	515.5	12700
5	0.0012	535.5	13050
6	0.0003	463.5	10900
7	0.0004	563.5	13280
8	0.0005	513.5	11990
9	0.0002	558.5	13240
11	0.001	559.5	13230
12	0.0008	401.5	9550 (data not used)

$$*\bar{\sigma}_T = 12610 \text{ psi}; V_\sigma = 5.8\%$$

2. Test Results

Each specimen failed with fracture occurring transverse to the applied stress direction which is typical for a brittle material. Of the eleven specimens tested, nine failed with fracture occurring well within the gage section length; one was marginal, having fractured within 1/16 inch of the fillet and one failed 1/8 inch into the fillet region. Measurements taken of the fractured diameters disclosed that the two specimens which failed in the region of the fillet were 0.001 inch and 0.0025 inch larger than their respective minimum diameters. Microscopic examination of the fractured zones did not reveal any large flaws which could initiate fracture in this region. A possible explanation to why the two specimens failed in the fillet region instead of at the minimum diameter could be that surface discontinuities were present which were undetected in the initial inspection; that is, annular scratches developed in the machining process. Data gathered from the test on the specimen which fractured close to the fillet were incorporated into the results, and the stress was based on the minimum cross-sectional area. Justification for using the minimum diameter is based on the fact that the minimum cross-sectional area had to sustain the total load imposed on the specimen even though fracture did not occur at that point.

The tensile strength computed from conditions of equilibrium was obtained from the knowledge of the pressure at failure, the dimensions of the specimen, a calibration constant, and is given by Eq. (1):

$$\sigma_T = p_f \left[\left(\frac{D}{d} \right)^2 - 1 \right] k \quad (1)$$

where k is the O-ring load-loss calibration constant. The value for k used in the calculations was 0.97. The data are tabulated in Table I.

The average tensile strength $\bar{\sigma}_T$ was computed from

$$\bar{\sigma}_T = \frac{\sum_{i=1}^n \sigma_{Ti}}{n} \quad (2)$$

The standard or root-mean-square deviation S_σ and the coefficient of variance V_σ of the tensile strength are calculated from

$$S_\sigma = \sqrt{\frac{\sum_{i=1}^n (\sigma_{Ti} - \bar{\sigma}_T)^2}{n}} \quad (3)$$

and

$$V_\sigma = \frac{100 S_\sigma}{\bar{\sigma}_T} \quad (4)$$

Table I exhibits the data collected.

3. Analysis of Test Results

To arrive at the average tensile strength and the coefficient of variance, data from only nine of the eleven test specimens were considered. The data of specimen No. 3 were discarded because failure occurred in the fillet region, even though the tensile strength value obtained, based on the minimum diameter, compared favorably with the average value. The data of specimen No. 12 was also discarded. Microscopic examination of the fractured surfaces revealed a flaw in the area of fracture initiation which would account for the low value of 9550 psi calculated for the tensile strength.

Results obtained varied from a low of 10,900 psi to a high of 13,280 psi with an average tensile strength value of 12,610 psi. (Data published by the Hysol Corporation list the average tensile strength for this material at 12,000 psi at 77°F.) The coefficient of variance was calculated to be less than 6 percent which is a good indication of uniformity of material and consistency

in the test procedure and equipment used. Data are not available from specimen No. 10, since this specimen was selected to be used as a transducer in the determination of the O-ring load loss.

VII. CONCLUSIONS

The test device is compact, portable, easy to use and, being of simple construction, is relatively inexpensive to manufacture. Alignment of the specimen, which is an ever-present problem in a conventional test system setup, is effectively controlled automatically in the test device, and reliable, consistent results are obtained dependent only on the quality of the specimen and material. From a review of the data compiled in the test program, it is quite obvious that consistent results were achieved using this test system. The problem encountered in machining a constant-diameter gage section was overcome by polishing the gage section length to a slightly reduced diameter at the middle of the section length. It would be advisable to incorporate this modification into the manufacture of future specimens provided the transition is made smoothly to avoid a notch effect. Unfortunately, funding was not available at this time to calibrate the O-ring load loss for a variety of brittle materials; but if the procedure outlined in Appendix A, para. A3 is followed, this data can be readily obtained in any future brittle material testing program. At the time of inception of this program, the authors deemed the hydraulic system outlined in Appendix C to be adequate for their needs. The system was a general purpose design, and some difficulties were experienced in using it. Fluctuations in the system caused variations in the stress rate of the test specimen. Even though it did not adversely affect the test program, it could create a problem in future work where a fine control of the stress rate is important. Also, as was reported in Appendix C, a close approximation to a constant stress rate was obtained in the upper half of the work range. Through the use of a specialized hydraulic system, a constant stress rate could be obtained over the full range and greater control of the stress rate could be maintained.

APPENDIX A

SYSTEM ERRORS

A1. Eccentricity Error Calculation

The bending stress σ_b created by an eccentric load P produces an error E_e defined as:

$$E_e = \sigma_b / \sigma_x, \quad (A1)$$

where σ_x can be further defined as:

$$\sigma_x = \frac{4P}{\pi d^2}. \quad (A2)$$

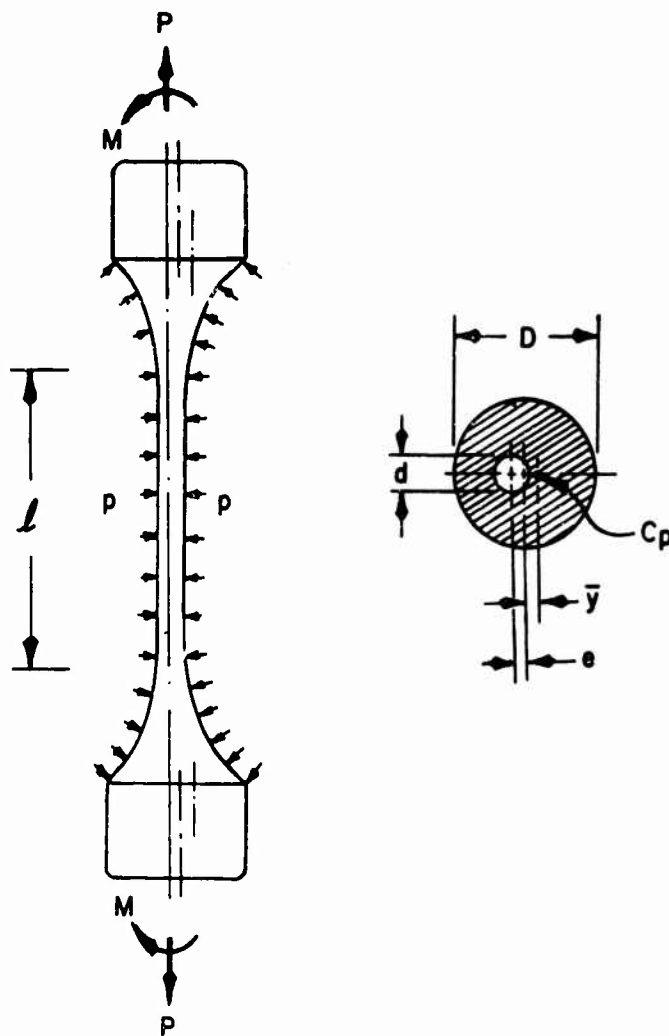


Figure A1 shows a specimen with an eccentricity between diameters and subjected to a pressure loading. The magnitude of eccentricity has been exaggerated for accentuation.

The pressure center C_p which is coincident with the centroid of the cross-hatched area in Figure A1 is located \bar{y} distance from the center line of D and is defined as:

$$\bar{y} = \frac{e}{\left(\frac{D}{d}\right)^2 - 1}. \quad (A3)$$

When pressure is applied, the resulting eccentric force creates an axial tensile force P and external couples M on the specimen. From Roark⁴,

$$M_{\max} = \frac{M}{\cosh \frac{l}{2} \sqrt{P/EI}} \quad (A4)$$

where $M = P (e + \bar{y})$.

Figure A1. Eccentric specimen

Combining Eqs. (A3) and (A4) results in

$$M_{\max} = \frac{Pc}{\left[1 - \left(\frac{d}{D}\right)^2\right] \cosh \frac{l}{2} \sqrt{P/EI}} \quad (A5)$$

In Eq. (A1), σ_b can be defined as

$$\sigma_b = \frac{M_{\max} c}{I} \quad (A6)$$

Substituting Eq. (A5) into Eq. (A6), replacing I with its value $\pi d^4/64$ and P with its value $\sigma_x \pi d^2/4$, and then substituting Eq. (A6) into Eq. (A1) results in:

$$E_e = \frac{8e}{d \left[1 - \left(\frac{d}{D}\right)^2\right] \cosh \frac{2l}{d} \sqrt{\frac{\sigma_x}{E}}} \quad (A7)$$

A2. Bending Errors

Eccentricity in the specimen between the gage section diameter and the end diameters can be an inherent error source in the system. Although each specimen was turned between centers, the eccentricity could only be held within a certain tolerance zone due to the limitations of the manufacturing process. As will be noted in Figure B3, the tolerance specified for concentricity was 0.0005 TIR. This tolerance was maintained in over 70 percent of the specimen tested with the worst condition encountered being 0.0012 inches total runout. Even an eccentricity of this magnitude produces an error of less than 1 percent as predicted by

$$\%E_e = \frac{8e}{d \left[1 - \left(\frac{d}{D}\right)^2\right] \cosh \frac{2l}{d} \sqrt{\frac{\sigma_x}{E}}} \times 100 \quad (A8)$$

An attempt was made to experimentally determine the possible combined bending error attributed to the eccentricity of the specimen and to any imposed bend force on the specimen created by inserting the specimen in the fixture. Four 350-ohm strain gages located 90° apart around the periphery of the middle portion of the gage section length were bonded to a 0.200-inch diameter specimen. This specimen was then inserted into the device along with a compensating dummy piece which had been machined to the same size gage-section diameter as that of the specimen. In this way, identical conditions of pressure and temperature would be imposed on specimen and dummy. Strain-gage wires were led out of the test device and sealed to prevent leakage in the hydraulic system. Each gage was individually connected to a BLH switching and balancing unit which, in turn, was connected to a BLH strain indicator. Each gage was balanced. An O-ring was placed over each end diameter of the specimen and the end caps assembled to the device to retain the O-rings. Hydraulic pressure was applied to the interior of the test device, and each gage was monitored to determine whether bending was occurring in the specimen. Readings obtained compared within 1-1/2 percent. It was concluded that inaccuracies in the strain gage measuring system could contribute this much variation, but nevertheless, the maximum bending expected should not exceed this value and in all probability would be much less.

A3. O-Ring Load Loss Calibration Procedure

The effect of the O-rings on the applied load to the specimen was experimentally determined by the following procedure:

An approximate pressure value to be used in the test device at a level fracture could be expected of the specimen was determined from a knowledge of the material's mechanical properties and the specimen geometry. It was in this range (approximately 500 psi) primarily that the effect of the O-rings was desired. Two specimens were used in this calibration procedure: the 0.200-inch diameter specimen used in the bending error test, and one which had been manufactured specifically for this test - a 0.312-inch gage section diameter specimen which met all the other dimensional requirements of the 0.200-inch diameter specimen. Strain gages were bonded to the 0.312-inch diameter in the same locations as were applied to the 0.200-inch diameter. The purpose of the 0.312-inch diameter specimen was to permit testing to a pressure of approximately 500 psi without exceeding a 1-percent strain to prevent damage to the strain gages. Because the pressure-displacement ratio would differ for the two specimens, the smaller diameter specimen would also be tested to a 1-percent strain, the data extrapolated to a value at 500 psi, and then compared to the data obtained at 500 psi of the 0.312-inch diameter specimen. Both specimens were calibrated to a 1-percent strain prior to testing in the test device to obtain a load-strain curve. Calibration was accomplished on conventional test equipment with the strain gages connected in series to determine axial strain only. With the 0.200-inch diameter specimen still in the test device upon conclusion of the bend error test, the strain gage leads were then connected in series and wired to the X axis of a Mosely 7001A X Y recorder. The test device pressure transducer was wired to the Y axis. (See Appendix C for Test Equipment and Measuring System.) Hydraulic pressure was again applied to the specimen and a series of tests conducted to obtain an average pressure-strain curve. Maximum pressure applied was slightly over 200 psi at an approximate stress rate of 800 psi/sec. This test procedure was repeated using the 0.312-inch diameter specimen and 0.312-inch diameter temperature-pressure compensating dummy to obtain a pressure-strain curve to approximately 475 psi. Repeatability of tests was within less than 1 percent for both specimens, and in both cases, the curves were essentially linear. Strain readings obtained experimentally from the two specimens were then extrapolated to 500 psi and each value compared to the predicted strain calculated from the equation:

$$\epsilon_p = P \left\{ \frac{1}{E_T} \left[\left(\frac{D}{d} \right)^2 - 1 \right] + \frac{1}{E_C} \right\}. \quad (A9)$$

The derivation of Eq. (A9) will be presented in a subsequent paragraph. As will be noted, this equation takes into consideration the pressure end effects on the temperature-pressure compensating dummy; therefore, the O-ring load loss can be determined through a comparison of experimental to predicted values.

E_C and E_T were experimentally determined. Some variation was found in the E_C test values by varying the stress rate of the tests. Therefore, the value obtained at a stress rate of 800 psi/sec was used in the calculations of Eq. (A9); however, even if the extreme experimental values of E_C were used in the equation, the change in contribution to the value of ϵ_p would be less than

0.5 percent. Tests conducted on the 0.200-inch diameter consistently indicated a value for E_T of approximately 3 percent higher than the results obtained from tests conducted on the 0.312-inch diameter specimen. This was probably due to a stiffening effect that the gages have upon the smaller diameter specimen. Because of this, the apparent elastic modulus found for each specimen was used in Eq. (A9) when comparing the predicted and extrapolated strain for each specimen. Comparative results indicated that the strain obtained experimentally from the 0.312-inch diameter specimen was 1-1/2 percent lower than the predicted result and the experimental strain of the 0.200-inch diameter specimen was 3 percent lower than the predicted result. Some of this variation between the two specimens may be attributable to extrapolation error. It can be concluded, however, that the error in tensile strength data, if the load loss due to the O-rings is ignored, should be not greater than 3 percent and more likely would be closer to the 1-1/2 percent figure.

Derivation of Eq. (A9) follows:

$$\epsilon_p = \epsilon_s - \epsilon_d \quad (A10)$$

where

$$\epsilon_d = \frac{\sigma_x}{E_c} - \frac{\sigma_y + \sigma_z}{E_c} \nu.$$

Substituting $-p$ for σ_x , σ_y , and σ_z , then

$$\epsilon_d = \frac{p(2\nu-1)}{E_c}. \quad (A11)$$

Also,

$$\epsilon_s = \frac{p}{E_T} \left[\left(\frac{D}{d} \right)^2 - 1 \right] + 2 \frac{p\nu}{E_c}. \quad (A12)$$

And substituting Eq. (A11) and (A12) into Eq. (A10) results in Eq. (A9).

A4. Triaxial Stress State

The stress state which existed in the BATT system also exists in the system presented here. The authors' reported on the possible error due to a deviation from a uniaxial stress state and made a comparison of each theory of failure as applied to a brittle material triaxially stressed to that of simple uniaxial tension to indicate the magnitude of the possible error. That discussion will be presented here again for the convenience of the reader. Only those theories of failure applicable to brittle failure will be considered and they are:

- a. Coulomb-Mohr theory of fracture⁵
- b. Pauli's⁶ modification of the Coulomb-Mohr theory,

- c. Griffith-Crowan⁷ criterion for fracture, and
- d. maximum normal stress theory.

The governing equation applied to the specimen during test according to the Coulomb-Mohr theory of fracture, considering the three principal stresses, is:

$$\sigma_x - \sigma_p = \sigma_T \quad (A15)$$

Since the applied hydrostatic pressure is to be ignored in the determination of the tensile strength, that is, $\sigma_T = \sigma_x$, the stress difference ratio $\Delta\sigma$, according to the Coulomb-Mohr theory, will be

$$\Delta\sigma = \frac{\sigma_T - \sigma_p}{\sigma_T} = \frac{\sigma_x - \sigma_p - \sigma_p}{\sigma_T} \quad (A16)$$

or

$$\frac{\sigma_x - \sigma_p}{\sigma_x - \sigma_p}$$

The axial stress σ_x across the gage section area is obtained by equilibrium of forces and is given by

$$\sigma_x = p \left[\left(\frac{D}{d} \right)^2 - 1 \right] k \quad (A17)$$

where k is a calibration constant for the load loss in the system caused by the contact between the O-rings and the specimen. The stress σ_p is equal to the hydrostatic pressure, that is, $-p$. Substituting for σ_x and σ_p in Eq. (A16) gives

$$\Delta\sigma = \frac{q}{k \left[\left(\frac{D}{d} \right)^2 - 1 \right] + q} \quad (A18)$$

From average typical properties* published for the material used in this study, $q = 0.7$ (from Figure 85), $D = 0.996$ inches, and $d = 0.2$ inches. The value for $k = 0.97$. Substitution of these values into Eq. (A18) results in an error of approximately 3 percent.

The modified Coulomb-Mohr theory, as suggested by Funi, results in the same identity as Eq. (A16) except that q is replaced by q' and is defined as

$$q' = \frac{1 - \sin \phi}{1 + \sin \phi}$$

*Data Sheet published by Hysol Corporation, Glean, New York

In the case where ϕ is unknown, limits on $\Delta\sigma$ can be determined by allowing ϕ to vary from zero, where tensile fracture occurs at 45° to the principal axis, to $\pi/2$, where fracture occurs transverse to the principal axis — the more realistic fracture for brittle materials and the type of fracture experienced here. Thus, when $\phi = 0$, $q' = 1$ and $\Delta\sigma \approx 4$ percent. When $\phi = \pi/2$, $q' = 0$ and $\Delta\sigma = 0$. In any event, therefore, if the hydrostatic component is ignored, the maximum error introduced will not exceed 4 percent. If the Griffith-Orowan criterion or the maximum normal stress theory dictates failure of a brittle material, then $\sigma_x = \sigma_T$, and the applied hydrostatic pressure can be ignored without error.

APPENDIX B

TEST DEVICE AND SPECIMEN

B1. Test Device

The compact, lightweight test device (Figures B1 and B2) was composed basically of a cylinder, end caps, and O-rings. The criteria for the multi-piece design was threefold: (a) to minimize the possibility of specimen damage when placing the specimen into the fixture; (b) to facilitate manufacture; and (c) ease of assembling the test device. A 1-inch bore was machined through the length of the 2-inch O.D., 4-1/4-inch long cylinder and held concentric to an external pilot diameter at each end of the cylinder. Similarly, in each end cap a 1-inch bore was machined to within 3/8 inch of the end face and held concentric to an internal pilot diameter. Mating of the pilot diameters maintained alignment of the cylinder and end cap bores. Threads machined forward of the pilot diameters provided the means of securing the end caps to the cylinder.

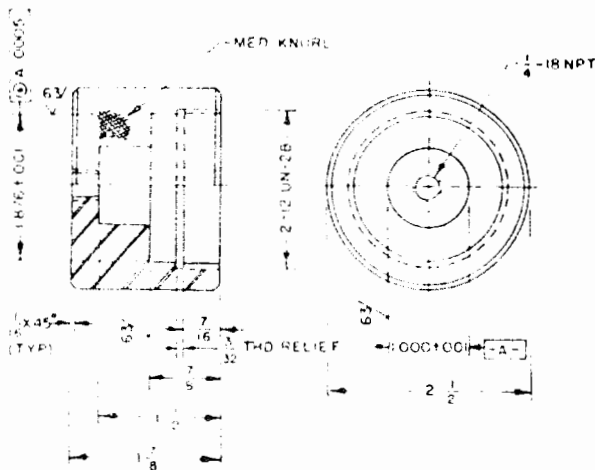


Figure B1. Test device end cap

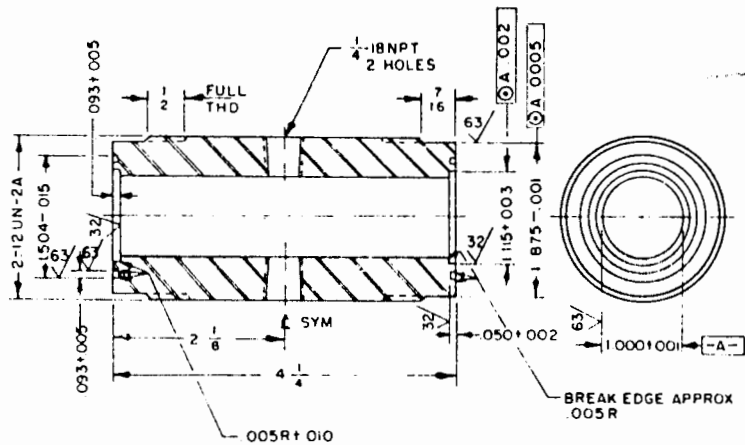


Figure B2. Test device cylinder

Assembly of the end caps to the cylinder was facilitated by cutting a diamond knurl into the O.D. of each end cap. A recess was machined at each end of the cylinder bore to accept the 0.070-inch cross-sectional diameter O-rings used to seal the end diameters of the specimen. Also, a groove was machined in each end face of the cylinder to accommodate a 0.070-inch cross-sectional diameter O-ring. The purpose of these O-rings is to provide a seal to prevent leakage between the threads of the end caps and cylinder during the set up procedure when the test device is pressurized without a specimen. In this way, adjustments can be made to the hydraulic pressure supply and test equipment without the danger of breaking a specimen prematurely. Two pipe ports, 180° apart, were machined in the middle portion of the cylinder to provide access to the interior of the test device for pressurizing and strain gaging. A pipe-threaded port was also machined through

the external face of each end cap to permit access to the interior of the test device and to provide a means of venting to eliminate back pressure during testing. A means of cushioning the specimens was necessary to prevent spalling of the fractured ends during testing. This was accomplished by inserting into the bore of each end cap a 1/8-inch thick soft rubber disk with a vent hole cut through the center. The hydraulic pressure inlet and the dynisco pressure transducer (Appendix C, para. C2) were connected to one of the cylinder ports. The other cylinder port was sealed with a pipe plug when not in use.

With the test device disassembled (end caps removed from the cylinder), the 4-3/4-inch long specimen (Figure B3) is easily slipped through the bore of the cylinder until approximately 1/4-inch length of specimen is protruding from each end of the cylinder. A silicon rubber O-ring with a 0.070-inch cross-section diameter is fitted over each end of the specimen and seated in the bore recess. Assembly of the end caps to the cylinder retain the specimen seals in position. Thus, specimen breakage is virtually eliminated using this test device whereas the possibility of breakage was ever present when inserting a specimen into the BATT.

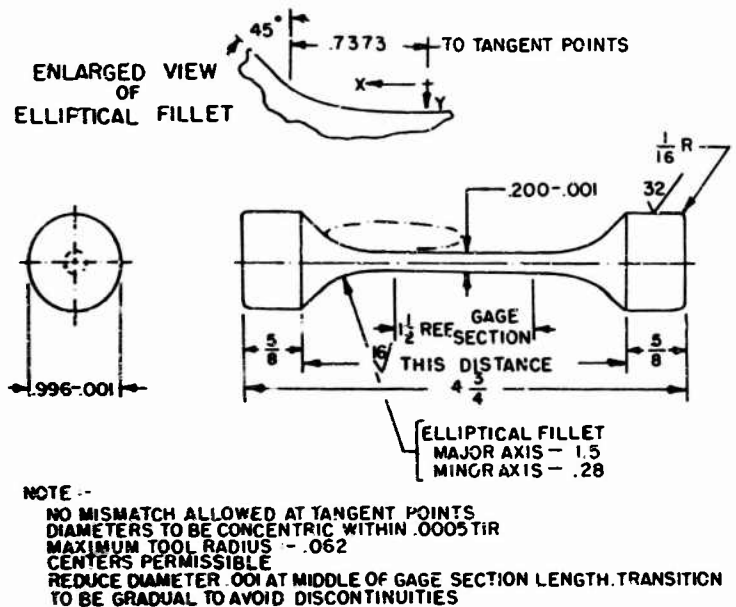


Figure B3. Test specimen configuration

B2. Specimen

In the tensile testing of ductile materials, a high degree of confidence that failure will occur in the constant diameter gage section can be assured by machining a generous fillet radius between the gage section and the larger end diameters of the test specimen. Although the radius is a potential stress raiser region, the inherent characteristic of a ductile material to yield locally and reduce the high stress concentration makes it possible to utilize this type of design. Brittle materials, on the other hand, do not respond in the same manner and so the design of the fillet region must be changed if a large percentage of failures are to occur within the gage section length. The ideal fillet would be one in which stress is constant along the entire profile. Preliminary testing of an elliptical fillet with a major axis of 1.5 inches and a minor axis of 0.28 inch produced favorable results; therefore, this fillet design was selected for the test specimen.

Twelve specimens were machined to the specifications of the design for brittle materials testing (Figure B3). Because of the method of testing, namely, the employment of a hydraulic fluid pressure to exert a tensile force on the gage section diameter, the basic configuration of the specimen was restricted to

a modified dumbbell type geometry. A 45° chamfer was machined tangent to the elliptical fillet and extended to the end diameter to facilitate manufacture and to permit the use of a turning tool with a 0.06-inch nose radius. All specimens were machined on a copy-type lathe using a master template, and the entire surface between end diameters was polished to a 16-rms value. An additional operation was later added to polish the gage-section diameter to a slight taper of 0.001 inch sloping toward the middle of the gage-section length. This was accomplished to induce failure at the minimum diameter gage section.

APPENDIX C

TEST EQUIPMENT AND MEASUREMENT SYSTEM

C1. Hydraulic Pump and Control System

Pressurizing of the fixture was accomplished through the use of a hydraulic pump available in the laboratory. The rated capacity of this piston-type pump was 0.8 gpm at 1200 rpm and 3000 psi. Power was supplied by a 220-volt, 60-cycle, 3-phase, 2-horsepower motor. To prevent pressure surging in the fixture and to minimize pressure pulsations, a one-pint piston-type accumulator was assembled in the pressure line. In series with the accumulator, a variable flow control valve and micrometer adjustment bypass valve was assembled to provide for a variable stress-time program for the specimens. An adjustable relief valve, set at a slightly higher pressure than the anticipated maximum required, protected the entire system from overload.

Flexibility and rapid disassembly of the test device was provided by a flexible line and a quick-release connection between the test device and power source. A variable pressure switch incorporated in the system and set at a low pressure of approximately 100 psi acted as a safety device in the event that the system was not manually shut down after fracture of the specimen. Overriding of this switch was accomplished by engaging the master on-button. Through experimentation, it was found that a gas charge of 90-psi pressure in the accumulator was the optimum pressure to allow a close approximation to a constant stress-rate curve in the upper half of the working range. Adjustment of the variable flow control and micrometer bypass valves established the stress rate at approximately 800 psi per sec.

C2. Measuring System

A dynisco flush diaphragm-type pressure transducer was used to record hydraulic pressure in the test device. Prior to assembling it to the device, the transducer was calibrated over its full range of 0-2000 psi. Calibration resistance values were also determined for use on an X-Y recorder to simulate pressure values. Auxiliary equipment used for calibration were: (a) Crosby fluid pressure scale; (b) BLH type 120 strain indicator; and (c) General Radio type 1432B decade box.

All fracture tests and load-loss tests were recorded on a Moseley 7001A X-Y recorder manufactured by Hewlett-Packard-Moseley. Accuracy was 0.2 percent of full scale for both axes, repeatability 0.1 percent on all ranges, and linearity 0.1 of full scale. Resolution was about 1/2 psi. Two decade resistance boxes in conjunction with two B&F instrument conditioning modules, Model No. 1-211A-1, which were electrically connected to the X-Y recorder, simulated pressure and strain gage resistance to the X and Y axes for periodic calibration. For fracture test recordings, the Y axis was set on 5 sec/in. calibrated range and the X axis calibrated for pressure recording. For load-loss testing, the X axis was converted to record strain values and the Y axis calibrated for pressure.

LITERATURE CITED

1. SEDLACK, R., and HALDEN, F. A. *Method of Tensile Testing of Brittle Materials*. Rev. Sci. Inst., v. 33, 1962, p. 298.
2. PEARS, C. D., and DIGESU, F. J. *Gas Bearing Facilities for Determining Axial Stress-Strain and Lateral Strain of Brittle Materials to 5500 F*. Proceedings, Am. Soc. for Testing and Mats., v. 65, 1965, p. 855.
3. BARATTA, F. I., and DRISCOLL, G. W. *A New Axial Tension Tester for Brittle Materials*. Army Materials and Mechanics Research Center, AMMRC TR 69-02.
4. ROARK, R. J. *Formulas for Stress and Strain*. McGraw-Hill Book Co. 4th edition, 1965, p. 150.
5. COULOMB, C. A. *Sur Une Application des Reyles de Maximio et Minimis a Quelques Problems de Statique Relatifo a l'Architecture*. Memoires de Mathematique et Physique, Academy Royal des Sciences, Par divers Savan, Amnee 1773, Paris, France, 1776.
6. PAUL, B. *A Modification of the Coulomb-Mohr Theory of Fracture*. Journal of Applied Mechanics, June 1961, p. 259.
7. OROWAN, E. *Fracture and Strength of Solids*. Reprinted from the Physical Society Report on Progress in Physics, v. XII, 1949, p. 185.